Mg/Ca ratios in coralline algae record northwest Atlantic temperature variations and North Atlantic Oscillation relationships

G. Gamboa,[1] J. Halfar,[1] S. Hetzinger,[1,2] W. Adey,[3] T. Zack,[4] B. Kunz,[4] and D. E. Jacob[4]

Received 12 March 2010; revised 9 August 2010; accepted 20 August 2010; published 17 December 2010.

[1] Climate variability in the North Atlantic has been linked in part to the North Atlantic Oscillation (NAO). The NAO influences marine ecosystems in the northwestern Atlantic and transport variability of the cold Labrador Current. Understanding historic patterns of NAO variability requires long-term and high-resolution climate records that are not available from instrumental data. Here we present the first century-scale proxy record of sea surface temperature (SST) variability from the Newfoundland shelf, a region from which other annual-resolution shallow marine proxies are unavailable. The 116 year record was obtained from three sites along the eastern Newfoundland shelf using laser ablation inductively coupled mass spectrometry–determined Mg/Ca ratios in the crustose coralline alga *Clathromorphum compactum*. The alga is characterized by a high Mg-calcite skeleton exhibiting annual growth increments and a century-scale lifespan. Results indicate positive correlations between interannual variations in Mg/Ca ratios and both station-based and gridded instrumental SST. In addition, the record shows high spatial correlations to SST across the Newfoundland shelf and the Gulf of St. Lawrence. Before 1950 the Mg/Ca proxy record reveals significant departures from gridded temperature records. While the Newfoundland shelf is generally considered a region of negative correlations to the NAO, the algal time series as well as a recent modeling study suggest a variable negative relationship with the NAO which is strongest after ~1960 and before the mid-1930s.

Citation: Gamboa, G., J. Halfar, S. Hetzinger, W. Adey, T. Zack, B. Kunz, and D. E. Jacob (2010), Mg/Ca ratios in coralline algae record northwest Atlantic temperature variations and North Atlantic Oscillation relationships, *J. Geophys. Res.*, *115*, C12044, doi:10.1029/2010JC006262.

1. Introduction

[2] The Labrador Current (LC), a cold and low-salinity water mass dominates the shelf and upper continental slope of Labrador and Newfoundland [*Petrie and Anderson*, 1983]. The LC originates from a combination of arctic water masses and the westward branch of the West Greenland Current in the Labrador Sea [*Lazier and Wright*, 1993]. Two main components characterize the LC: (1) a surface inshore branch flowing on the continental shelf, and (2) the offshore branch, which travels along the upper continental slope (Figure 1) [*Petrie and Anderson*, 1983]. The LC has an important cooling effect on the Canadian Atlantic provinces affecting ocean productivity by changing the physical and biological properties of the seawater [*Petrie and Drinkwater*, 1993; *Colbourne et al.*, 1997; *Drinkwater and Mountain*, 1997]. Changes in temperature and salinity of the LC are partly the result of interannual and long-term conditions driven by the North Atlantic Oscillation (NAO [see *Reverdin et al.*, 1997]). The NAO is the key indicator of atmospheric variability for middle and high latitudes influencing the North Atlantic Ocean [*Visbeck et al.*, 2001; *Hurrell et al.*, 2003; *Polyakova et al.*, 2006; *Petrie*, 2007]. When the NAO index is positive, northwesterly winds are stronger, northwestern Atlantic water temperatures become colder, and the area of sea ice expands and extends further to the south. The Labrador Sea and northwestern Atlantic slope water temperature history resembles the mirror image of the NAO index with a 1 or 2 year lag [*Curry and McCartney*, 2001; *Pershing et al.*, 2001; *Petrie*, 2007]. This is due to vertical mixing processes allowing ocean temperature anomalies created over a deep mixed layer in winter to be preserved below the surface in summer and reappear at the surface in the following fall [*Alexander and Deser*, 1995]. Warm, salty (cold, fresh) conditions prevail on the Newfoundland-Labrador shelf and the Gulf of St. Lawrence during periods of negative (positive) NAO anomalies, while the opposite pattern is observed south of this region [*Pershing et al.*, 2001; *Petrie*, 2007]. In fact,

[1]CPS Department, University of Toronto at Mississauga, Mississauga, Ontario, Canada.
[2]Now at Leibniz Institute of Marine Sciences at University of Kiel (IFM-GEOMAR), Kiel, Germany.
[3]Department of Botany, Smithsonian Institution, Washington, D. C., USA.
[4]Earth System Science Research Centre, Department of Geosciences, Johannes Gutenberg Universität, Mainz, Germany.

0148-0227/10/2010JC006262

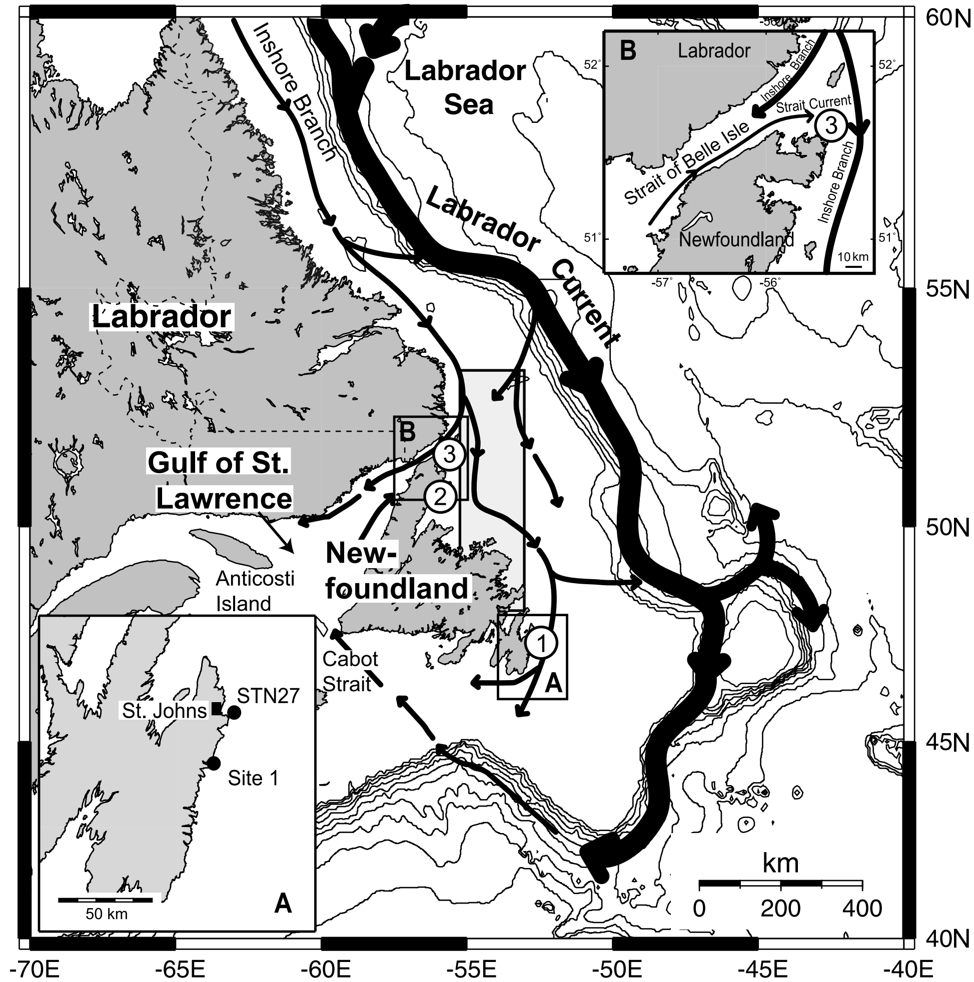

Figure 1. Location map showing sampling sites: (1) Bay Bulls, Newfoundland; (2) Cape St. Martin, Newfoundland; and (3) Quirpon Island, Newfoundland. Heavy lines associated with the Labrador Current indicate deep offshore branch, and thin lines indicate shallow inshore branch. Gray box indicates area used for calculating instrumental ERSST time series. Flow path of the Labrador Current is from *Colbourne et al.* [1997] and *Han* [2004]. (a) Location of oceanographic station 27 with respect to site 1. (b) Oceanography in Strait of Belle Isle and location of site 3.

ocean temperatures off the central Newfoundland shelf showed minima in the early 1970s, mid-1980s and early 1990s when the NAO index was high [*Parsons and Lear*, 2001; *Colbourne*, 2004].

[3] While the overall view of the NAO affecting the temperature and salinity distributions on the Canadian Atlantic continental shelf is compelling, it needs to be recognized that many of the individual correlations are neither large nor persistent [*Petrie*, 2007]. In fact, correlations of the NAO index with annual air temperature anomalies off St. John's, Newfoundland, have not always been significant during the past century [*Polyakova et al.*, 2006; *Petrie*, 2007]. In addition, surface ocean conditions are only weakly related to NAO patterns as the magnitudes of the correlations of the winter NAO and annual temperature anomalies generally increase from the surface and have a maximum value at or near the bottom [*Petrie*, 2007]. The most striking feature of the summer temperature structure on the Newfoundland shelf is the large volume of the subsurface cold intermediate layer with a maximum vertical extent of over 200 m. This cold, relatively fresh subpolar shelf water in turn is isolated from the warmer and saltier water of the continental slope [*Colbourne*, 2004]. Hence, the above demonstrates that Newfoundland shelf SSTs are not representative of the entire water column. While many studies assume a steady relationship between the NAO and North Atlantic SST, recent work suggests that this relationship is highly variable [*Polyakova et al.*, 2006]. Nonlinear dynamics with the NAO have been shown in multicentury time series of land surface temperatures from Europe [*Slonosky et al.*, 2001] and of Arctic sea ice export through Fram Strait [*Peterson et al.*, 2003; *Schmith and Hansen*, 2003; *Rogers et al.*, 2004].

[4] Hence, the influence of the NAO in the subarctic northwest Atlantic is still under debate [*Polyakova et al.*, 2006; *Petrie*, 2007]. This is largely due to the fact that long-term local time series of in situ oceanographic observations are confined to the second half of the 20th century with most hydrographic observations becoming available only from the 1970s on [*Colbourne and Fitzpatrick*, 2003; *Petrie*, 2007; *Hughes et al.*, 2009]. Reconstructing marine

Table 1. Site Information for *C. compactum* Specimens Collected Off Newfoundland, Canada[a]

Sample	Site	Location	Latitude (°N)	Longitude (°W)	Period Analyzed
SJ28-L1	Bay Bulls, St. John's	Newfoundland	47°18.496′	52°47.354′	1917–2006
SJ28-L2	Bay Bulls, St. John's	Newfoundland	47°18.496′	52°47.354′	1913–2006
SJ21-L1	Bay Bulls, St. John's	Newfoundland	47°18.496′	52°47.354′	1918–2006
SJ21-L2	Bay Bulls, St. John's	Newfoundland	47°18.496′	52°47.354′	1918–2006
QP4–3-L1	Quirpon Island	Newfoundland	51°35.135′	55°25.490′	1931–2006
QP4–3-L2	Quirpon Island	Newfoundland	51°35.135′	55°25.490′	1931–2006
170716	Cape St. Martin	Newfoundland	50°1.5′	55°53′	1890–1963

[a]L1 and L2 refers to two different transect lines on a single sample.

conditions and climate in the Canadian Atlantic back to the 19th century, a time that is generally regarded as delimiting the onset of large-scale human-induced impacts on natural systems, is of utmost importance to better understand the NAO-SST relationship and predict future environmental changes [*Kushnir*, 1994]. This is especially true if one wants to relate climate variability off Newfoundland to marine ecosystem changes, such as the dramatic late 1990s decline in cod abundance [*Parsons and Lear*, 2001; *Drinkwater*, 2002, 2006].

[5] Here the crustose coralline alga *Clathromorphum compactum* was used as an archive of Newfoundland shelf sea surface temperatures. A number of studies during the past decade have demonstrated that middle- and high-latitude crustose coralline algae are an emerging extratropical marine climate archive as they are among the longest-lived shallow marine organisms with life spans of several hundred years [*Halfar et al.*, 2000, 2007, 2008; *Frantz et al.*, 2005; *Kamenos et al.*, 2008]. Coralline algae display well developed annual growth increments in a high Mg-calcite skeleton. Early studies have found cyclic variations of Mg content in crustose coralline algae as a response to seasonal changes in ocean temperatures [*Chave and Wheeler*, 1965; *Moberly*, 1968; *Milliman et al.*, 1971]. The feasibility of using coralline algal Mg/Ca relationships for environmental reconstructions was later demonstrated during yearlong field calibration studies conducted in cold-temperate oceans (Gulf of Maine and Scotland; see *Halfar et al.* [2008] and *Kamenos et al.* [2008]). The *Halfar et al.* [2008] calibration study demonstrated a slowdown in winter growth of *C. compactum*. It was further shown that areas of high Mg values within the skeleton of two species of *Clathromorphum* typically occur during the period of summer growth [*Hetzinger et al.*, 2009, 2010]. In addition, the robustness of using algal Mg/Ca ratios as environmental indicators was substantiated by Synchrotron Mg-X-ray absorbance near edge spectroscopy that indicates that Mg is indeed associated with the calcite lattice [*Kamenos et al.*, 2009]. All these characteristics along with the absence of a slowdown of growth with increasing ontogenetic age, which is common in other extratropical marine calcifiers such as bivalves, make crustose coralline algal Mg/Ca ratios suitable for reconstructions of SST.

[6] *C. compactum*, the subject of this study, is widely distributed on rocky substrates along coastlines of the boreal-subarctic North Atlantic, the northern Pacific, and even extending into the Arctic Ocean [*Adey*, 1965; *Adey et al.*, 2008]. *C. compactum* thrives in water temperatures <16°C and occurs from 1 to 40 m water depth reaching its maximum abundance around 8 m [*Adey*, 1965]. Mean annual growth rates of *C. compactum* in Newfoundland are 250–360 μm [*Halfar et al.*, 2010]. As individual dome-shaped plants attain a thickness of up to 3 cm off Newfoundland, *C. compactum* can reach a lifespan of ~100 years.

[7] The aim of this paper is to provide a record of sea surface temperatures in the Labrador Current (LC) region to 1890 using Mg/Ca ratios from *C. compactum*. This is the first century-scale time series of Mg/Ca variations in the crustose coralline *C. compactum* and the first annual-resolution shallow marine proxy record from the Labrador Current Inshore Branch region on the Newfoundland shelf.

2. Methods

[8] Living plants of *C. compactum* were collected from hard substrate via SCUBA at three localities along the eastern coastline of Newfoundland (Table 1). One specimen was obtained from a museum collection established in 1964 (U.S. National Herbarium of the Smithsonian Institution, Washington DC) and 3 specimens were collected in August 2008 at two locations in Newfoundland (see Figure 1 and Table 1). Samples collected in 2008 were from 10 m depth, whereas collection information for the 1964 sample indicates a depth of 3–10 m. All locations are within the influence of the Labrador Current (LC).

[9] The air-dried *C. compactum* specimens were slabbed vertically parallel to the direction of growth to a thickness of about 1 cm using a rock saw, then thick sections (2 mm) were cut from the slabs. The sample surface was polished following a standard protocol involving manual and machine-based polishing steps to 1 μm. Digital images of the polished surface were produced using an Olympus reflected light microscope (BX51) attached to an automated sampling stage/imaging system equipped with the software geo.TS (Olympus Soft Imaging Systems). This setup allows two-dimensional mapping of the surfaces of polished specimens at various magnifications. The resulting high-resolution photomosaics enabled the identification of growth patterns over the entire sample and the subsequent selection of sampling locations (Figure 2a). Mg/Ca ratios were obtained by laser ablation inductively coupled plasma mass spectrometry (LA-ICP-MS). In preparation for LA-ICP-MS analysis, paths for laser line transects as well as two reference points per sample were digitized on photomosaics along the direction of growth using geo.TS software (Figure 2a). Care was taken to avoid areas of growth disruptions and small unconformities. Coordinates of digitized paths and reference points were subsequently transferred to the LA-ICP-MS system. After recoordination of the sample, laser line transects could be precisely positioned and analyzed along previously digitized paths.

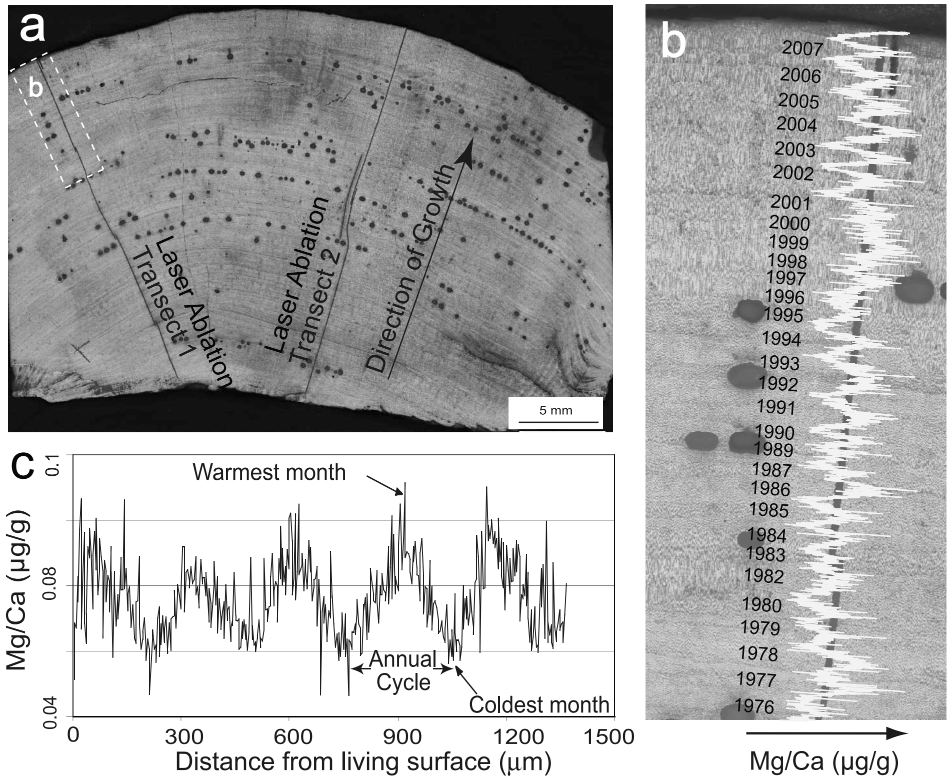

Figure 2. (a) Cross section of *C. compactum* showing position of laser ablation inductively coupled plasma mass spectrometry transects perpendicular to growth increments. (b) Detailed view of annual Mg/Ca cycles superimposed on sectioned specimen and used to establish the age model. (c) Laser ablation inductively coupled plasma mass spectrometry–measured Mg/Ca cycles used for calculating annual growth increment widths.

[10] Mg and Ca concentrations were measured using an Agilent 7500ce Quadrupole ICP-MS coupled to a New Wave Research UP-213 laser ablation system (213 nm wavelength, Nd:YAG Laser; see *Jacob* [2006]) at the Department of Geosciences, Johannes Gutenberg-Universität Mainz, Germany. Measurements were carried out with laser energy densities of 6 J/cm^2 and helium as carrier gas. Transects measuring up to 6000 μm in length were analyzed with a scan speed of 10 μm/second, a spot size of 65 μm and 10 Hz pulse rate. The cycling rate of the ICP-MS was set at scan intervals of 3.29 scans/second, resulting in a sampling resolution of 3.044 μm along the continuously measured line transect. Here ^{43}Ca was used as the internal standard with calcium concentrations measured by ICP-OES [*Hetzinger et al.*, 2009]. NIST (U.S. National Institute of Standard and Technology Standard Reference Material) SRM 610 glass reference material was used as external standard. Independent measurements of NIST SRM 610 were used to confirm that instrument drift was insignificant. Data for NIST SRM 610 were taken from the GeoReM database (K. P. Jochum and F. Nehring, GeoReM preferred values, 2006; see http://georem.mpch-mainz.gwdg.de/sample_query_pref.asp). Relative standard deviation (RSD) for repeated analysis of NISTSRM610 (external reproducibility) is 0.67% for ^{24}Mg/^{43}Ca. Detection limits were: ^{24}Mg = 0.16 ppm, ^{43}Ca = 54.9 ppm; 1-sigma error from repeated analysis of NBS610: ^{24}Mg = 3.4%, ^{43}Ca = 3.1%. Mg/Ca are reported as mass ratios (μg/g)/(μg/g) which can be converted to molar ratios (mol/mol) by dividing ratios by 0.60644.

[11] Since all samples were live collected, the top layer was assigned the year of collection. Age models and sample ages shown in Table 1 were established on the basis of the pronounced seasonal cycle in algal Mg/Ca. Previous studies on coralline algae have shown that areas of low (high) Mg values within the skeleton typically occur during the period of reduced (main) growth in late winter (summer) and are interpreted to correspond to winter (summer) values [*Halfar et al.*, 2008; *Hetzinger et al.*, 2009]. Minimum (maximum) Mg/Ca values were tied to March (August), which is on average the coolest (warmest) month at the study sites (Figures 2b and 2c). The algal Mg/Ca time series were linearly interpolated between these anchor points using the AnalySeries software [*Paillard et al.*, 1996] to obtain an equidistant proxy time series with 12 samples/year resolution. Except for sample 170716 which only allowed for positioning one laser profile, two Mg/Ca transects were analyzed on each sample in order to reduce intraspecimen variability. Variability within the same specimen can arise owing to internal growth irregularities caused by grazing damage (e.g., sea urchins, chitons; see *Steneck* [1983]). The two transects were then averaged to create a combined single Mg/Ca data set for that specimen. Values were normalized by subtracting the

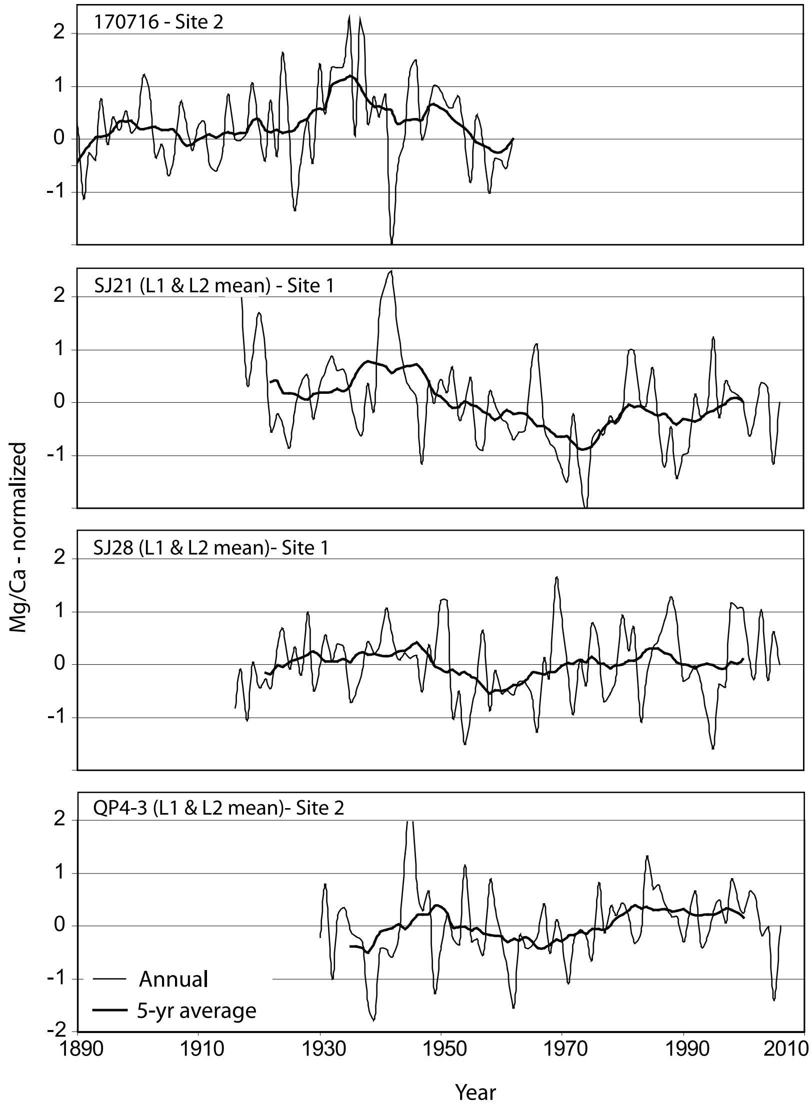

Figure 3. Mg/Ca records from individual samples indicate site-specific variability.

mean of each transect and dividing by the standard deviation. Each transect spans between 75 and 93 years in length (Table 1). Site similarities for overlapping portions of time series (annual data, linear trend removed) are as follows: sites 1–2: $r = 0.31$, $n = 34$, $p < 0.06$; sites 1–3: $r = 0.45$, $n = 65$, $p < 0.001$, sites 2–3: $r = 0.29$, $n = 32$, $p < 0.1$; SJ 21. Correlations of two transects within individual samples are SJ 21, $r = 0.42$, $n = 88$, $p < 0.0001$; SJ 28, $r = 0.16$, $n = 90$, $p < 0.1$; QP 43, $r = 0.1$, $p < 0.4$. Individual correlations are weak or nonsignificant and therefore transects from all 4 samples from three sites were combined into a Mg/Ca master chronology based on ages assigned for each individual sample (Figure 3). This reduces site and sample-specific noise, enhances the common climate signal and is similar to methodology commonly employed when analyzing terrestrial and marine biogenic proxy archives [*Black et al.*, 2009]. Averaged values for the overlapping periods were obtained by calculating the arithmetic mean for each year.

[12] Instrumental temperature time series from 1950 onward were obtained from oceanographic station 27 (0 m water depth), which is located about 7 km off St. John's Harbor (www.dfo-mpo.gc.ca; see Figure 1). Additional instrumental observations were retrieved from gridded SST data available from the National Oceanic and Atmospheric Administration Extended Reconstructed Sea Surface Temperature version 3 data set (NOAA ERSST.v3; see *Smith et al.* [2008]) for the 47–53°N, 53–55°W grid (Figure 1). Spatial and running correlations with the NOAA ERSST.v3 data set and the NAO winter (December through March) index were conducted using the tool Climate Explorer (http://climexp.knmi.nl; see *van Oldenborgh et al.* [2009]). The NAO winter index is based on the difference of normalized sea level pressure (SLP) between Lisbon, Portugal and Stykkisholmur/Reykjavik, Iceland [*Hurrell et al.*, 2003]. Correlation with the NAO index assumes a 2 year lag [see *Alexander and Deser*, 1995]. Air temperatures at St. Johns (47.62°N, 52.73°E) were obtained from http://www.meds-sdmm.dfo-mpo.gc.ca/isdm-gdsi/azmp-pmza/climat/airTemp-fra.asp?stn=StJohns, whereas air temperatures from

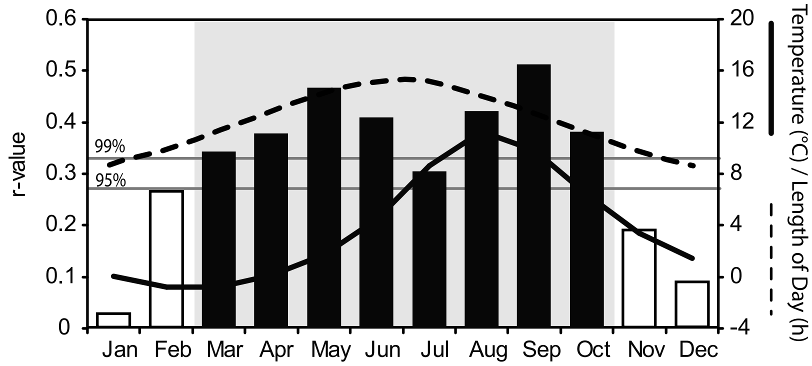

Figure 4. Correlation of annually averaged Mg/Ca ratios of *C. compactum* (average sites 1–3) with monthly instrumental sea-surface temperatures (ERSST) from 1950 to 2004 (vertical bars). In addition, monthly ERSST sea-surface temperatures and length of day are shown. Significant correlations (>95%) indicate that Mg/Ca temperature relationships are strongest between March and October (gray area). Open bars indicate months of insignificant correlations.

Anticosti Island were obtained from http://climexp.knmi.nl/. The linear trend has been removed in both data sets.

3. Mg/Ca Temperature Relationship

[13] A comparison of annual Mg/Ca ratios averaged from sites 1–3 (master chronology) to monthly instrumental SST anomalies between 1950 and 2004 (ERSST data set) delimits the months of significant Mg/Ca-temperature relationships (Figure 4). Results show that Mg/Ca ratios record March to October sea surface temperatures on the Newfoundland shelf (95% significant). Strongest correlations are observed between April–June and August–October (99% significant), while correlations during July are somewhat weaker. The winter months from November to February exhibit no significant correlation with algal Mg/Ca, indicating that calcification is significantly reduced or comes to a halt during the cold and dark winter months. It has been shown in earlier studies that algal calcification rates are influenced by both light and temperature [*Adey*, 1970]. While the winter months exhibit low light and temperature conditions, Newfoundland shelf temperatures remain suppressed well into April, with average ambient temperatures around freezing (Figure 4). Hence, data here suggest that significant calcification takes place in March and April despite low temperatures, but with increasing amounts of solar radiation available. Furthermore, reduced correlations in midsummer might be related to short-term mixing events due to southwesterly winds where cold water masses from below the shallow thermocline influence surface temperature conditions, and therefore algal Mg/Ca ratios (Figure 4). This is in contrast to algal growth rates measured in specimens of *C. compactum* from Newfoundland, which are highest between July and September [*Halfar et al.*, 2008]. The subannual Mg-temperature relationship presented here also differs from an oxygen isotope-based growth model of *C. compactum* from the Gulf of Maine that indicated a significant temperature signal being recorded from May–December only [*Halfar et al.*, 2010] . Reasons for the difference can be (1) growth of the Maine specimens near the southern limit of the biogeographical distribution of the species, (2) low sampling resolution for oxygen isotopes resulting in a loss of detail and thus influencing the isotope-temperature relationship. While an improved temperature growth and Mg/Ca relationship can only be established by mesocosm experiments under controlled conditions, the present data point to brief episodes of upper ocean mixing in the summer and a lack of growth and Mg/Ca incorporation during the winter months. The relationship established in Figure 4 forms the basis for delimiting correlative analyses with instrumental SST time series data in this study to the March–October period.

4. Comparison to Instrumental Temperatures

[14] A comparison of the annual-resolution Mg/Ca time series from site 1 (average of samples SJ-21 and SJ-28, two transects/sample) to a nearby station-based instrumental SST record (station $27_{\mathrm{Mar-Oct}}$, 0 m water depth; see Figure 1) from 1950 to 2004 indicates strong positive correlations based on annual data ($r_{annual} = 0.51$, $p < 0.001$; see Figure 5a). The standard error (RMSE) of the annual Mg/Ca site 1 time series and station $27_{\mathrm{Mar-Oct}}$ is 0.24, indicating tightly clustered values around the regression line ($y = 0.3195x - 1.6906$) and a highly accurate index. Station 27, which is located about 30 km from the sampling site, records water properties of the inshore branch of the Labrador Current and is one of the most frequently monitored hydrographic stations in the northwest Atlantic (Figure 1) [*Colbourne et al.*, 1997; *Colbourne and Fitzpatrick*, 2003; *Hughes et al.*, 2009]. Variations in water properties at station 27 are representative of conditions across a broad area of the Newfoundland shelf [*Petrie et al.*, 1981; *Colbourne and Fitzpatrick*, 2003]. Hence, correlations of the site 1 Mg/Ca proxy time series with station 27 SST (Figure 5a) confirm the value of using algal Mg/Ca ratios as temperature proxies for the Newfoundland shelf. Similar results are obtained when the Mg/Ca master chronology is compared to ERSST for the period 1950–2004 (spatially averaged data from 46°N–52°N and 55°W–50°W; $r_{annual} = 0.59$, $p < 0.001$, RMSE = 0.17; see Figure 5b). This grid was selected as a close representation of water mass characteristics of the inshore branch of the LC. While ERSST data from this grid and station 27 (0 m) are well correlated (1950–2004; $r_{annual} = 0.67$, $p < 0.001$), it needs to be kept in mind that the ERSST data exhibit greater variability than the in situ station

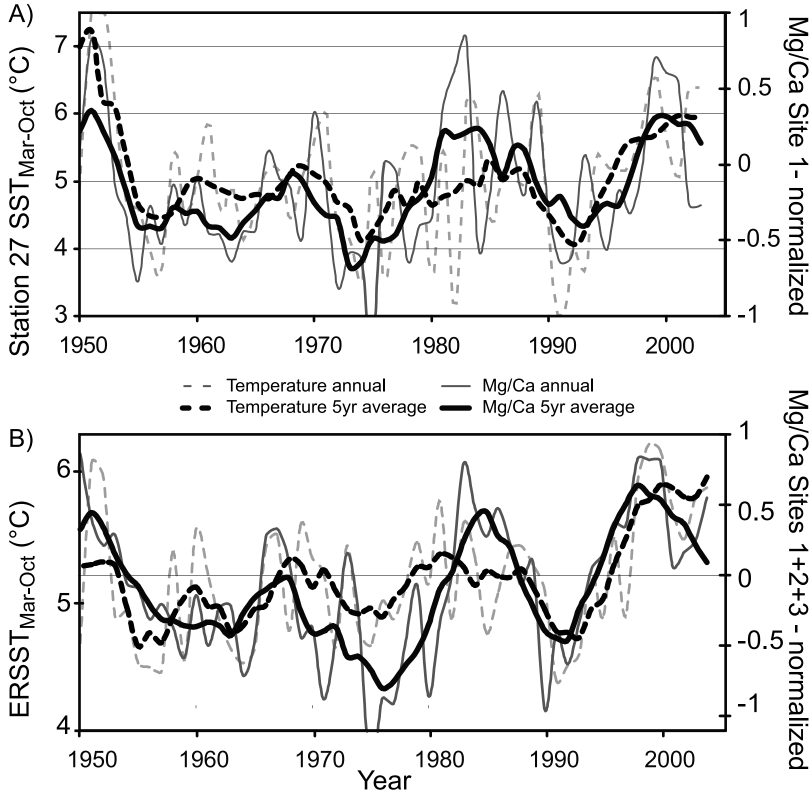

Figure 5. (a) Time series of Mg/Ca ratios of site 1 (average of samples SJ-21 and SJ-28, two transects/sample) and instrumental temperatures at station 27 (0 m depth; 1950–2004); $r_{annual} = 0.51$, $p < 0.001$. (b) Time series of Mg/Ca ratios of sites 1, 2, and 3 (average of samples SJ-21, SJ-28, QP4–3, and 170716) and $ERSST_{Mar–Oct}$ (47–53°N, 53–55°W; 1950–2004); $r = 0.59$, $p < 0.001$.

27 data on interannual time scales [*Hughes et al.*, 2009]. Correlations between ERRST data derived from a grid near station 27 (51–53°W; 47–49°N) and station 27 (1950–2004; $r_{annual} = 0.73$, $p < 0.001$) and the site 1 Mg/Ca time series (1950–2004, $r_{annual} = 0.64$, $p < 0.001$) are similar. In summary, the comparison of annual algal Mg/Ca data with station 27 and ERSST demonstrates that the algal time series provides a robust record of temperature characteristics of the Labrador Current inshore branch.

5. Spatial Correlation of Mg/Ca With SST

[15] Significant spatial correlations of the annual algal Mg/Ca master chronology (1950–2004) to large-scale SST variability are observed within the path of the Labrador Current inshore branch extending into the Gulf of St. Lawrence (Figure 6). In fact, the master chronology is weakly related to an air temperature record from 1890 to 1954 from Anticosti Island, a region of highly significant spatial correlations (Figures 1 and 7). The semienclosed Gulf of St. Lawrence communicates directly with the Labrador Current region through Cabot Strait between Newfoundland and Nova Scotia, and to a lesser degree through the Strait of Belle Isle between Newfoundland and Labrador (Figure 1) [*Han*, 2004]. In addition, water mass export from the Gulf of St. Lawrence takes place via the Strait Current along the southeast side of the Strait of Belle Isle [*Garrett and Petrie*, 1981]. At site 3 mixing takes place between the cold water masses associated with the inshore branch of the LC and the warm outflow of the Strait Current at the Strait of Belle Isle. Until further samples become available from the Gulf of St. Lawrence, reasons for spatial correlations being highest with a region in the western Gulf of St. Lawrence remain unexplained.

6. Extended Mg/Ca and ERRST Time Series

[16] While the Mg/Ca master chronology is well correlated to gridded ERSST data from 1950 onward, correlations are generally poor between 1890 and 1950 (Figure 8). These departures coincide with scarcity of observations available for compiling the ERSST monthly temperature reconstruction, which is largely model derived in the first half of the 20th century owing to insufficient sampling and bias uncertainty (for a detailed discussion, see *Smith et al.* [2008]). In fact, number of observations for the selected grid were <20/month prior to 1950 and generally <5/month prior to 1940 (Figure 8a). In order to fill the data-sparse periods before ~1950, reconstruction techniques are used in compiling the ERSST data set. These assess the pattern of spatial variability from recent periods with good data coverage and use these patterns to fill gaps in earlier periods of sparse observations [*Hughes et al.*, 2009]. When observations are sparse over spatially extensive areas such as the subarctic northwest Atlantic, the reliability of the reconstruction suffers, as at any particular time a large part of the data set is

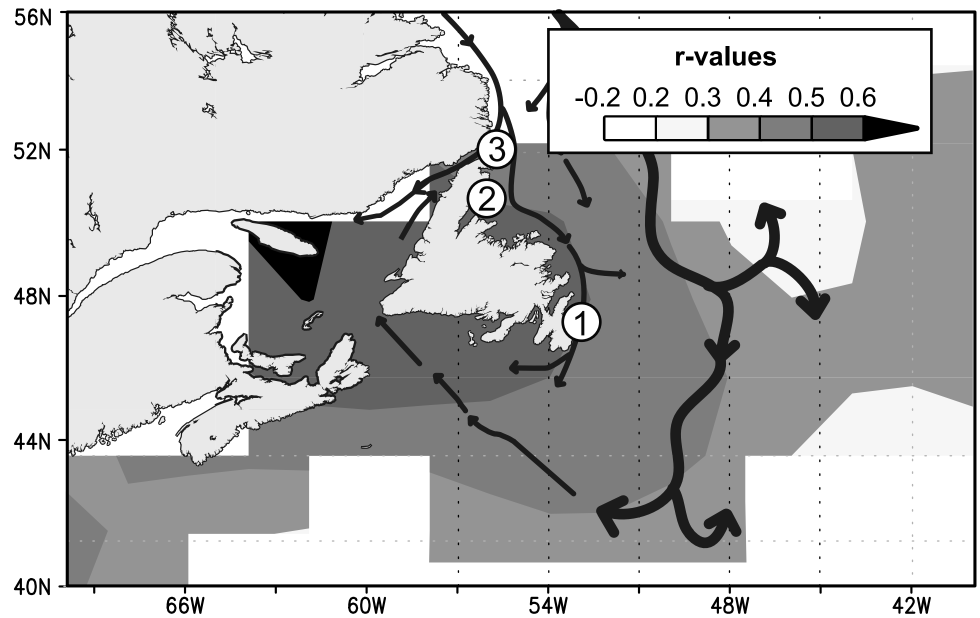

Figure 6. Spatial correlation of annual Mg/Ca time series averaged from three sites and NOAA $ERSST_{Mar-Oct}$ data (1950–2004). Location of three sampling sites and major currents indicated.

reconstructed [*Hughes et al.*, 2009]. The lack of data in the pre-1950s ERSST reconstruction is also evident from a comparison with air temperature records (Figure 7).

[17] A running correlation (see Figure 8 for description of correlation parameters) showing temporal variations in the relationships between the algal Mg/Ca master chronology and ERSST data highlights significant departures in the time series prior to 1950 coinciding with the period of sparse observational data (Figure 8b). While the master chronology is compiled of multiple samples from three sites, before 1918 the time series combines only two sites and only one site prior to 1913. Hence, robustness of the master chronology decreases before 1918 with cycle amplitudes increasing owing to reduced sample numbers.

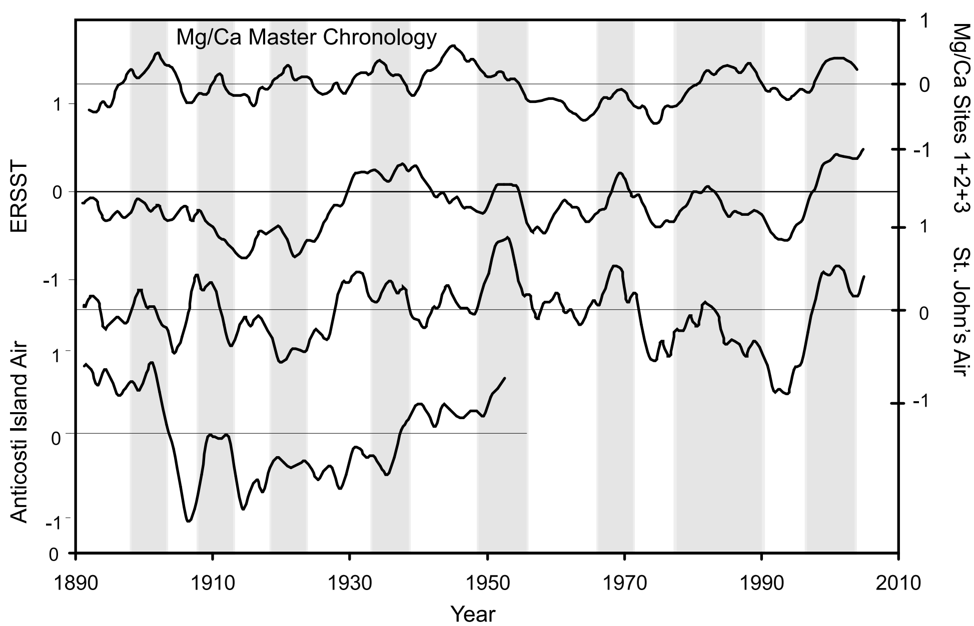

Figure 7. Comparison of Mg/Ca master chronology with instrumental air temperature records from St. John's (47.62°N, 52.73°E; 1890–1987) and ERSST (47–53°N, 53–55°W) (normalized, linear trend removed from all data sets). Note common positive anomalies of master chronology with air temperature indices (shaded gray) and poor comparison to ERRST before 1950. Positive Mg/Ca anomalies in 1940s show no correspondence with ERSST or St. John's air temperature data, but Anticosti Island time series indicates warming. Long-term warming in Anticosti starting in mid-1930s is not observed in other records.

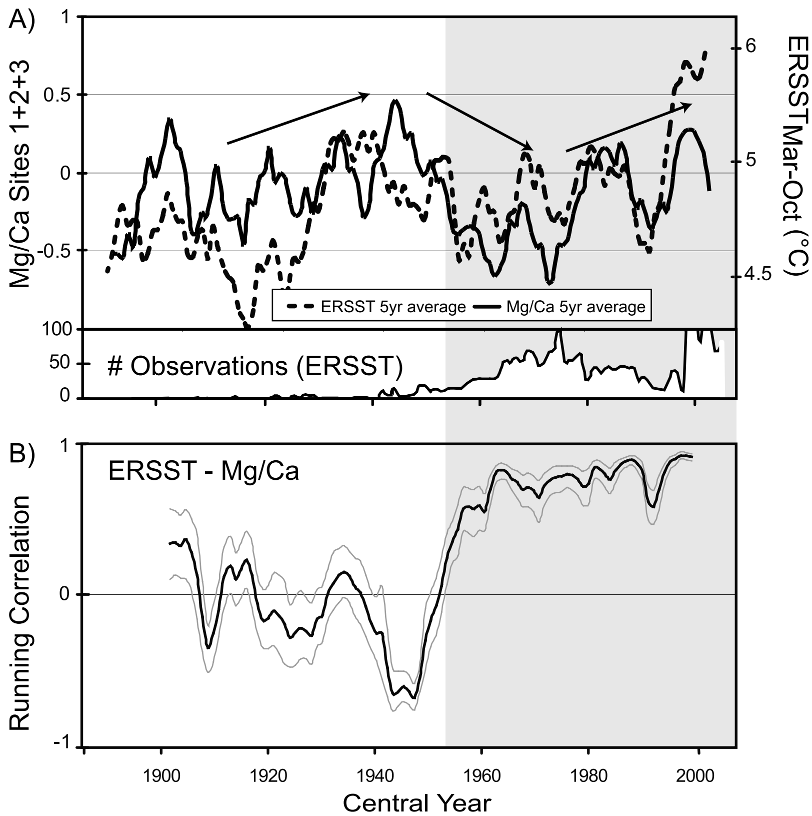

Figure 8. (a) Five year averaged Mg/Ca ratios of sites 1, 2, and 3 (master chronology; 1890–2004) compared to $ERSST_{Mar–Oct}$ (47–53°N, 53–55°W; $r_{annual} = 0.24$, $p < 0.01$, $n = 115$; $r_{5\ year\ average} = 0.37$, $p = 0.08$; p value adjusted for loss of degrees of freedom). In addition, the number of monthly observations in ERSST instrumental data for temperature field used in this study (47–53°N, 53–55°W) is shown. Note the limited observations prior to 1950. (b) Running correlation coefficients (21 year sliding window) between $ERSST_{Mar–Oct}$ and Mg/Ca time series shown in Figure 8a for the time period 1890–2004. Upper and lower 95% confidence limits (thin lines) are calculated with bootstrap methods (1000 sample Monte Carlo). Correlation coefficients are plotted at center of each 21 year period. Gray area indicates period of significant correlation between $ERSST_{Mar–Oct}$ and master chronology.

[18] The Mg/Ca chronology reflects the main trends of 20th century North Atlantic climate such as a warming period between the 1920s and 1940s. This warming trend, which is well documented in the Arctic [*Bengtsson et al.*, 2004] has been linked to ecosystem shifts in marine species throughout the North Atlantic [*Drinkwater*, 2006]. In contrast to the uniform post-1918 warming trend of the ERSST record, warming until the early 1940s is expressed in a step-like pattern in the Mg/Ca time series and the air-temperature records (Figure 7). Prior to this period ERSST data indicate a strong cooling from 1900 to 1920 that surpasses the cooling in the 1950s and 1960s. However, there are no reports of ecosystem changes associated with this apparent cooling and no consistent anomalies are observed in the NAO during this time (Figure 9). The algal Mg/Ca record instead indicates only minor cooling. Hence, in the absence of evidence for a significant early 20th century cooling episode or ecosystem changes in the northwestern Atlantic, the cooling of Newfoundland SST indicated by ERSST might in fact have been less pronounced. The second half of the 20th century shows a distinctive pattern of decadal-scale Mg/Ca fluctuations corresponding to changes in SST. The 1950s and 1960s are characterized by a cooling trend represented in the master chronology as decreasing Mg/Ca values. From the 1970s onward, Mg/Ca ratios display positive anomalies, except for a period of decreasing Mg/Ca ratios in the early 1990s, which is in line with observational data.

7. Comparison With NAO

[19] Correlations of both regional $ERSST_{Mar–Oct}$ and the Mg/Ca master chronology with the NAO (2 year lag, winter index; see *Hurrell et al.* [2003]) are variable between 1890 and 2004 (Figure 9). Both time series show strong negative correlations with the NAO from the 1960s onward. Between the mid-1930s and ~1960 correlations are insignificant or positive in both, $ERSST_{Mar–Oct}$ data and the Mg/Ca master chronology. Prior to the mid-1930s correlations between the Mg/Ca master chronology and the NAO are significantly negative, whereas the $ERSST_{Mar–Oct}$ only partly exhibit significant correlations with NAO. Except for the pre-1905 portion of the record, high correlations between the Mg/Ca master chronology and the NAO coincide with positive phases of the NAO. Hence, the generally positive phase of the NAO from the 1910s to 1940 and the 1970s onward has influenced algal Mg/Ca ratios and therefore water temperatures along the

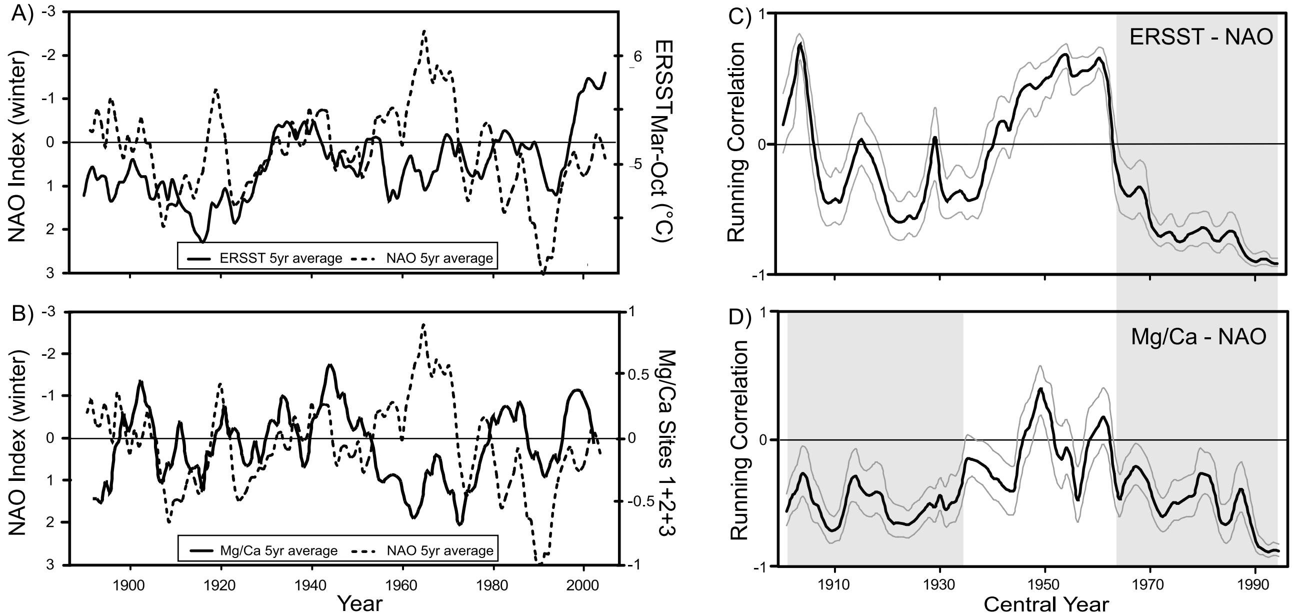

Figure 9. Comparison between the (a) 5 year averaged winter NAO index [*Hurrell et al.*, 2003] and $ERSST_{Mar–Oct}$ (47–53°N, 53–55°W) and (b) Mg/Ca ratios of master chronology (no lag). (c and d) Running correlations (2 year lag) of the time series in Figures 9a and 9b (same method as in Figure 8). Note significant negative correlations of Mg/Ca and ERSST with NAO after the early 1960s (gray box), and before the mid-1930s (Mg/Ca time series only).

Newfoundland-Labrador shelf. The influence of the NAO on Newfoundland shelf water temperatures is particularly significant for the post 1960 period, when the phase of the NAO has been shifting from mostly negative to mostly positive index values [*Visbeck et al.*, 2001; *Hurrell et al.*, 2003]. In summary, the above shows (1) that the Mg/Ca master chronology reveals a higher correlation to the NAO than the regional ERSST time series, and (2) that the influence of the NAO on the Newfoundland shelf has been highly variable over time.

[20] A variable NAO-SST relationship has been proposed by a number of authors [*Slonosky et al.*, 2001; *Schmith and Hansen*, 2003; *Polyakova et al.*, 2006]. Spatial correlations of the NAOm index (the mobile North Atlantic Oscillation as defined by *Portis et al.* [2001]) and Atlantic-wide SST indicate that the Newfoundland-Labrador Region has experienced major temporal fluctuations with respect to positive and negative signs of the correlations [*Polyakova et al.*, 2006]. While the time slice from 1910 to 36 is dominated by strong negative NAO correlations on the Newfoundland-Labrador shelf, the 1937–1963 period is characterized by weak correlations of a positive sign [*Polyakova et al.*, 2006]. Hence, the relationship between the NAO and SST varies over time and changes occur in conjunction with low-frequency (decadal or multidecadal) climate variability in the North Atlantic. Decades of strong correlations alternate with decades of insignificant or even opposite sign correlations [*Polyakova et al.*, 2006]. The algal proxy time series presented here confirms this alternating relationship with periods of negative correlations in the 20th century separated by a multidecadal episode of weakly positive correlations from the mid-1930s to the 1960s. Hence, the Mg/Ca time series demonstrates that, when evaluating the influence of the NAO on Newfoundland shelf oceanography, ecosystems and fisheries [*Drinkwater*, 2002; *Petrie*, 2007], the fluctuating association with the NAO has to be taken into account.

8. Conclusions

[21] This is the first study using LA-ICP-MS-determined Mg/Ca ratios of the crustose coralline algae *C. compactum* as recorders of SST dynamics in the northwest Atlantic. Combining Mg/Ca data from modern and museum-collected specimens from multiple sites along the eastern Newfoundland shelf yielded a 116 year master chronology. The annually resolved Mg/Ca time series is temporally and spatially correlated with local and regional instrumental SST after 1950. Before 1950 instrumental SST observations off the eastern coastline of Newfoundland are sparse and are poorly related to the algal proxy time series. A comparison with the NAO exhibits periods of alternating positive and negative correlations with the proxy record showing dominantly negative correlations in the early and late 20th century separated by a period of weak positive correlations from the mid-1930s to the 1960s. Hence, the often discussed negatively correlated influence of the NAO affecting SST, fisheries and ecosystems on the Newfoundland shelf has fluctuated in the past, with negative NAO anomalies being strongly correlated to high SST anomalies on the Newfoundland shelf. Weak or positive NAO anomalies in turn are characterized by variable SST anomalies. While the algal Mg/Ca time series presented here allows for evaluating ocean variability over the past century, further analyses of museum collected specimens are expected to provide a robust record of Newfoundland shelf SST well into the 19th century.

[22] **Acknowledgments.** We thank Wade Saunders, Bob Hooper from Bonne Bay Marine Station, and Philip Sargent from Memorial University of Newfoundland for logistical support and advice on sampling locations. J.H. was supported by a Natural Sciences and Engineering Research Council of Canada Discovery grant and by a Canadian Foundation for Climate and Atmospheric Sciences grant (Gr-7004). S.H. acknowledges support from the Alexander von Humboldt Foundation (Feodor Lynen Fellowship). This is a Geocycles publication.

References

Adey, W. H. (1965), The genus *Clathromorphum* (Corallinaceae) in the Gulf of Maine, *Hydrobiologia*, *26*, 539–573, doi:10.1007/BF00045545.

Adey, W. H. (1970), The effects of light and temperature on growth rates in boreal-subarctic crustose corallines, *J. Phycol.*, *6*, 269–276.

Adey, W. H., S. C. Lindstrom, M. H. Hommersand, and K. M. Müller (2008), The biogeographic origin of Arctic endemic seaweeds: A thermogeographic view, *J. Phycol.*, *44*, 1384–1394, doi:10.1111/j.1529-8817.2008.00605.x.

Alexander, M. A., and C. Deser (1995), A mechanism for the recurrence of wintertime midlatitude SST anomalies, *J. Phys. Oceanogr.*, *25*, 122–137, doi:10.1175/1520-0485(1995)025<0122:AMFTRO>2.0.CO;2.

Bengtsson, L., V. A. Semenov, and O. M. Johannessen (2004), The early twentieth-century warming in the Arctic—A possible mechanism, *J. Clim.*, *17*, 4045–4057, doi:10.1175/1520-0442(2004)017<4045:TETWIT>2.0.CO;2.

Black, B. A., C. A. Copenheaver, D. Frank, M. J. Stuckey, and R. E. Kormanyos (2009), Multi-proxy reconstructions of northeastern Pacific sea surface temperature data from trees and Pacific geoduck, *Palaeogeogr. Palaeoclimatol. Palaeoecol.*, *278*, 40–47, doi:10.1016/j.palaeo.2009.04.010.

Chave, K. E., and B. D. Wheeler Jr. (1965), Mineralogic changes during growth in the red alga *Clathromorphum compactum*, *Science*, *147*, 621, doi:10.1126/science.147.3658.621.

Colbourne, E. B. (2004), Decadal changes in the ocean climate in Newfoundland and Labrador waters from the 1950s to the 1990s, *J. Northwest Atl. Fish. Sci.*, *34*, 43–61, doi:10.2960/J.v34.m478.

Colbourne, E. B., and C. Fitzpatrick (2003), Station 27 oceanographic monitoring station—A long history, *Atl. Zone Monit. Program Bull.*, *3*, 18–21.

Colbourne, E. B., B. deYoung, S. Narayanan, and J. Helbig (1997), Comparison of hydrography and circulation on the Newfoundland shelf during 1990–1993 with the long-term mean, *Can. J. Fish. Aquat. Sci.*, *54*, 68–80, doi:10.1139/cjfas-54-S1-68.

Curry, R. G., and S. McCartney (2001), Ocean gyre circulation changes associated with the North Atlantic Oscillation, *J. Phys. Oceanogr.*, *31*, 3374–3400, doi:10.1175/1520-0485(2001)031<3374:OGCCAW>2.0.CO;2.

Drinkwater, K. (2002), A review of the role of climate variability in the decline of Northern Cod, *Am. Fish. Soc. Symp.*, *31*, 113–130.

Drinkwater, K. (2006), The regime shift of the 1920s and 1930s in the North Atlantic, *Prog. Oceanogr.*, *68*, 134–151.

Drinkwater, K. F., and D. B. Mountain (1997), Climate and oceanography, in *Northwest Atlantic Groundfish: Perspectives on a Fishery Collapse*, edited by J. G. Boreman et al., pp. 3–25, *Am. Fish. Soc.*, Bethesda, Md.

Frantz, B. R., M. S. Foster, and R. Riosmena-Rodríguez (2005), *Clathromorphum nereostratum* (Corallinales, Rhodophyta): The oldest alga? *J. Phycol.*, *41*, 770–773, doi:10.1111/j.1529-8817.2005.00107.x.

Garrett, C., and B. Petrie (1981), Dynamical aspects of the flow through the Strait of Belle Isle, *J. Phys. Oceanogr.*, *11*, 376–393, doi:10.1175/1520-0485(1981)011<0376:DAOTFT>2.0.CO;2.

Halfar, J., T. Zack, A. Kronz, and J. Zachos (2000), Geochemical signals of rhodoliths (coralline red algae)—A new biogenic archive, *J. Geophys. Res.*, *105*, 22,107–22,116, doi:10.1029/1999JC000128.

Halfar, J., R. Steneck, B. R. Schöne, G. W. K. Moore, M. M. Joachimski, A. Kronz, J. Fietzke, and J. A. Estes (2007), Coralline alga reveals first marine record of subarctic North Pacific climate change, *Geophys. Res. Lett.*, *34*, L07702, doi:10.1029/2006GL028811.

Halfar, J., R. S. Steneck, M. Joachimski, A. Kronz, and A. D. Wanamaker Jr. (2008), Coralline red algae as high-resolution climate recorders, *Geology*, *36*, 463–466, doi:10.1130/G24635A.1.

Halfar, J., S. Hetzinger, W. H. Adey, T. Zack, G. Gamboa, B. Kunz, B. Williams, and D. E. Jacob (2010), Coralline algal growth-increment widths archive North Atlantic climate variability, *Palaeogeogr. Palaeoclimatol. Palaeoecol.*, doi:10.1016/j.palaeo.2010.04.009, in press.

Han, G. (2004), Sea level and surface current variability in the Gulf of St. Lawrence from satellite altimetry, *Int. J. Remote Sens.*, *25*, 5069–5088, doi:10.1080/01431160410001709039.

Hetzinger, S., J. Halfar, A. Kronz, R. Steneck, W. H. Adey, P. A. Lebednik, and B. R. Schöne (2009), High-resolution Mg/Ca ratios in a coralline red algae as a proxy for Bering Sea temperature variations from 1902 to 1967, *Palaios*, *24*, 406–412, doi:10.2110/palo.2008.p08-116r.

Hetzinger, S., et al. (2010), High-resolution analysis of trace elements from the North Atlantic and North Pacific in encrusting coralline algae by laser ablation ICP-MS, *Palaeogeogr. Palaeoclimatol. Palaeoecol.*, doi:10.1016/j.palaeo.2010.06.004, in press.

Hughes, S. L., N. P. Holliday, E. B. Colbourne, V. Ozhigin, H. Valdimarsson, S. Osterhus, and K. Wiltshire (2009), Comparison of in situ time-series of temperature with gridded sea surface temperature datasets in the North Atlantic, *ICES J. Mar. Sci.*, *66*, 1467–1479, doi:10.1093/icesjms/fsp041.

Hurrell, J. W., Y. Kushnir, G. Ottersen, and M. Visbeck (2003), An overview of the North Atlantic Oscillation, in *The North Atlantic Oscillation: Climatic Significance and Environmental Impact*, *Geophys. Monogr. Ser.*, vol. 134, edited by J. W. Hurrell et al., pp. 1–35, AGU, Washington, D. C.

Jacob, D. E. (2006), High sensitivity analysis of trace element poor geological reference glasses by laser-ablation inductively coupled plasma mass spectrometry (LA-ICP-MS), *Geostand. Geoanal. Res.*, *30*, 221–235, doi:10.1111/j.1751-908X.2006.tb01064.x.

Kamenos, N., M. Cusack, and P. G. Moore (2008), Coralline algae are global paleothermometers with bi-weekly resolution, *Geochim. Cosmochim. Acta*, *72*, 771–779, doi:10.1016/j.gca.2007.11.019.

Kamenos, N., M. Cusack, T. Huthwelker, P. Lagarde, and R. E. Scheibling (2009), Mg-lattice associations in red coralline algae, *Geochim. Cosmochim. Acta*, *73*, 1901–1907, doi:10.1016/j.gca.2009.01.010.

Kushnir, Y. (1994), Interdecadal variations in North Atlantic sea surface temperature and associated atmospheric conditions, *J. Clim.*, *7*, 141–157, doi:10.1175/1520-0442(1994)007<0141:IVINAS>2.0.CO;2.

Lazier, J. R. N., and D. G. Wright (1993), Annual velocity variations in the Labrador Current, *J. Phys. Oceanogr.*, *23*, 659–678, doi:10.1175/1520-0485(1993)023<0659:AVVITL>2.0.CO;2.

Milliman, J. D., M. Gastner, and J. Mueller (1971), Utilization of magnesium in coralline algae, *Geol. Soc. Am. Bull.*, *82*, 573–580, doi:10.1130/0016-7606(1971)82[573:UOMICA]2.0.CO;2.

Moberly, R., Jr. (1968), Composition of magnesian calcites of algae and pelecypods by electron microprobe analysis, *Sedimentology*, *11*, 61–82, doi:10.1111/j.1365-3091.1968.tb00841.x.

Paillard, D., L. Labeyrie, and P. Yiou (1996), Macintosh program performs time series analysis, *Eos Trans. AGU*, *77*(39), 379, doi:10.1029/96EO00259.

Parsons, L. S., and W. H. Lear (2001), Climate variability and marine ecosystem impacts: A North Atlantic perspective, *Prog. Oceanogr.*, *49*, 167–188, doi:10.1016/S0079-6611(01)00021-0.

Pershing, A. J., C. H. Greene, C. Hannah, D. Sameoto, P. S. Head, D. G. Mountain, J. W. Jossi, M. C. Benfield, P. C. Reid, and T. G. Durbin (2001), Oceanographic responses to climate in the northwest Atlantic, *Oceanography*, *14*, 76–82.

Peterson, K. A., J. Lu, and R. J. Greatbatch (2003), Evidence of nonlinear dynamics in the eastward shift of the NAO, *Geophys. Res. Lett.*, *30*(2), 1030, doi:10.1029/2002GL015585.

Petrie, B. (2007), Does the North Atlantic Oscillation affect hydrographic properties on the Canadian Atlantic Continental Shelf? *Atmos. Ocean*, *45*, 141–151, doi:10.3137/ao.450302.

Petrie, B., and C. Anderson (1983), Circulation on the Newfoundland Continental Shelf, *Atmos. Ocean*, *21*, 207–226.

Petrie, B., and K. Drinkwater (1993), Temperature and salinity variability on the Scotian Shelf and in the Gulf of Maine 1945–1990, *J. Geophys. Res.*, *98*, 20,079–20,089, doi:10.1029/93JC02191.

Petrie, B., B. Toulany, and C. Garrett (1981), The transport of water, heat and salt through the Strait of Belle Isle, *Atmos. Ocean*, *26*, 234–251.

Polyakova, E. I., A. G. Journel, I. V. Polyakov, and U. S. Bhatt (2006), Changing relationship between the North Atlantic Oscillation and key North Atlantic climate parameters, *Geophys. Res. Lett.*, *33*, L03711, doi:10.1029/2005GL024573.

Portis, D. H., J. E. Walsh, M. E. Hamly, and P. J. Lamb (2001), Seasonality of the North Atlantic Oscillation, *J. Clim.*, *14*, 2069–2078, doi:10.1175/1520-0442(2001)014<2069:SOTNAO>2.0.CO;2.

Reverdin, G., D. Cayan, and Y. Kushnir (1997), Decadal variability of hydrography in the upper northern North Atlantic in 1948–1990, *J. Geophys. Res.*, *102*, 8505–8531, doi:10.1029/96JC03943.

Rogers, J. C., S.-H. Wang, and D. H. Bromwich (2004), On the role of the NAO in the recent northeastern Atlantic Arctic warming, *Geophys. Res. Lett.*, *31*, L02201, doi:10.1029/2003GL018728.

Schmith, T., and C. Hansen (2003), Fram Strait ice export during the nineteenth and twentieth centuries reconstructed from a multiyear sea ice index from southwestern Greenland, *J. Clim.*, *16*, 2782–2791, doi:10.1175/1520-0442(2003)016<2782:FSIEDT>2.0.CO;2.

Slonosky, V. C., P. D. Jones, and T. D. Davies (2001), Atmospheric circulation and surface temperature in Europe from the 18th century to 1995, *Int. J. Climatol.*, *21*, 63–75, doi:10.1002/joc.591.

Smith, T. M., R. W. Reynolds, T. C. Peterson, and J. Lawrimore (2008), Improvements to NOAA's historical merged land-ocean surface temperature analysis (1880–2006), *J. Clim.*, *21*, 2283–2296, doi:10.1175/2007JCLI2100.1.

Steneck, R. (1983), Escalating herbivory and resulting adaptive trends in calcareous algal crusts, *Paleobiology*, *9*, 44–61.

van Oldenborgh, G. J., S. S. Drijfhout, R. van Ulden, R. Haarsma, A. Sterl, W. Severijns, W. Hazeleger, and H. A. Dijkstra (2009), Western Europe is warming much faster than expected, *Clim. Past*, *5*, 1–12, doi:10.5194/cp-5-1-2009.

Visbeck, M., J. W. Hurrell, L. Polvani, and H. M. Cullen (2001), The North Atlantic Oscillation: Past, present and future, *Proc. Natl. Acad. Sci. U. S. A.*, *98*, 12,876–12,877, doi:10.1073/pnas.231391598.

W. Adey, Department of Botany, Smithsonian Institution, 10th and Constitution Ave., N W, Washington, DC 20560-0166, USA. (adeyw@si.edu)

G. Gamboa and J. Halfar, CPS Department, University of Toronto at Mississauga, 3359 Mississauga Rd., N, Mississauga, ON L5L 1C6, Canada. (jochen.halfar@utoronto.ca; steffen.hetzinger@utoronto.ca; gimy.gamboa@utoronto.ca)

S. Hetzinger, Leibniz Institute of Marine Sciences at University of Kiel (IFM-GEOMAR), Wischhofstr. 1-3, D-24148 Kiel, Germany.

D. E. Jacob, B. Kunz, and T. Zack, Earth System Science Research Centre, Department of Geosciences, Johannes Gutenberg Universität, Becherweg 21, D-55099 Mainz, Germany. (zack@uni-mainz.de; bkunz@students.uni-mainz.de; jacobd@uni-mainz.de)